Multi-scale kinetics of a field-directed colloidal phase transition

James W. Swan[a], Paula A. Vasquez[a], Peggy A. Whitson[b], E. Michael Fincke[b], Koichi Wakata[b], Sandra H. Magnus[b], Frank De Winne[c], Michael R. Barratt[b], Juan H. Agui[d], Robert D. Green[d], Nancy R. Hall[d], Donna Y. Bohman[d], Charles T. Bunnell[e], Alice P. Gast[f], and Eric M. Furst[a,1]

[a]Department of Chemical and Biomolecular Engineering and Center for Molecular and Engineering Thermodynamics, Allan P. Colburn Laboratory, 150 Academy Street, University of Delaware, Newark, DE 19716; [b]NASA Johnson Space Center, 2101 NASA Parkway, Houston, TX 77058; [c]European Space Agency, Linder Hoehe, 51147 Cologne, Germany; [d]NASA Glenn Research Center, 21000 Brookpark Road, Cleveland, OH 44135; [e]Zin Technologies Inc., 6745 Engle Road, Cleveland, OH 44130; and [f]Lehigh University, Office of the President and Department of Chemical Engineering, 27 Memorial Drive West, Bethlehem, PA 18015

Edited by William R. Schowalter, Princeton University, Princeton, NJ, and approved August 22, 2012 (received for review April 25, 2012)

Polarizable colloids are expected to form crystalline equilibrium phases when exposed to a steady, uniform field. However, when colloids become localized this field-induced phase transition arrests and the suspension persists indefinitely as a kinetically trapped, percolated structure. We anneal such gels formed from magneto-rheological fluids by toggling the field strength at varied frequencies. This processing allows the arrested structure to relax periodically to equilibrium—colloid-rich, cylindrical columns. Two distinct growth regimes are observed: one in which particle domains ripen through diffusive relaxation of the gel, and the other where the system-spanning structure collapses and columnar domains coalesce apparently through field-driven interactions. There is a stark boundary as a function of magnetic field strength and toggle frequency distinguishing the two regimes. These results demonstrate how kinetic barriers to a colloidal phase transition are subverted through measured, periodic variation of driving forces. Such directed assembly may be harnessed to create unique materials from dispersions of colloids.

magneto-rheological fluid | microgravity science | complex fluids

Smart fluids, colloidal dispersions actuated by external magnetic or electric fields, have diverse applications. In buildings, magneto-rheological (MR) dampers are used to absorb the energy of earthquakes, automobiles and trucks are equipped with active MR shock absorbers, and electro-rheological (ER) fluids enable haptic controllers and tactile displays in microelectronics devices. It is the ability to rapidly and reversibly change the rheological properties of smart fluids that makes them so attractive. Understanding the mechanisms that govern the formation and dissolution of structures in such materials is essential (1, 2). Field-induced interactions between particles is the primary mechanism of ER and MR fluids, and is driven chiefly by the mutual attraction or repulsion of induced dipoles.

Upon application of a steady field, ER and MR fluids respond by forming particulate chains along the field direction, imparting enhanced viscosity and the ability to resist transverse mechanical stresses. Following chain formation, thermal fluctuations create lateral attractive forces between neighboring chains and cause microstructural coarsening (3–5). Continued cross-linking between chains eventually damps the thermal fluctuations that drive coarsening in a self-retarding fashion. A kinetically arrested percolated structure results. However, investigations of the equilibrium thermodynamic properties of dipolar fluids show that the coarsened state is actually an arrested phase transition. Such dipolar fluids are predicted to form two coexisting phases: a particle rich, body-centered-tetragonal crystalline phase and a dilute fluid phase (6, 7). This contradiction with experimental observation is due to kinetic limitations; at typical field strengths (tens to hundreds of times stronger than the Boltzmann energy) the time scales over which the coarsened cross-linked intermediate would coalesce into the crystalline phase are longer than those over which reasonable experimental controls and measurements can be made.

Beyond smart fluids, similar arrested phase transitions arise in a colloidal suspension when sufficiently strong attractive interactions occur between particles (8–13). Like the percolated structures in MR and ER fluids, colloidal gels are elastic solids; their properties and stability are important in many industries. Despite the similarities, however, the kinetic arrest of the coarsened state of MR fluids can be circumvented, as Promislow and Gast (14, 15) demonstrate, by periodically toggling the magnetic field off and on. In the context of colloidal gelation, this is similar to instantaneously changing the system temperature (relative to the attractive interaction energy). During the field-off phase, free Brownian motion of the colloids results in a degradation of cross-linked chains and relaxation to lower energy microstructures. In their experiments, after approximately one hour in the pulsed field, the suspension relaxed into ellipsoidal- or columnar-like aggregates. This low energy phase of the MR fluid consists of compressible aggregates with a volume fraction determined by the balance between the confining pressure exerted by the magnetic attractions and the osmotic pressure of their constituent particles (16). Furthermore, the shape of these structures is determined by the field-induced dipolar forces; in particular, a competition between the demagnetizing field which favors elongation, and the aggregate surface energy, which favors sphericity (14, 17).

In previous work and similar studies involving magneto-rheological fluids (18–20), sedimentation of the colloidal particles obscures a complete picture of field-induced phase separation. For this reason, studies in microgravity offer a unique opportunity to interrogate the structural evolution, pattern formation, and aggregation dynamics of dipolar suspensions. The work presented here is an effort to examine fundamental aspects of MR fluid aggregation in pulsed magnetic fields without the influence of gravity. The distinguishing element of the present experiments is the duration over which the field-directed process is observed. Unlike other experiments, gravity does not cause the colloids to sediment to the boundaries of the experimental vessel. Solvent flows (hydrodynamics) and thermodynamic interactions (bound-

Author contributions: P.A.V., J.H.A., R.D.G., N.R.H., D.Y.B., C.T.B., A.P.G., and E.M. Furst designed research; P.A.W., E.M. Fincke, K.W., S.H.M., F.D., and M.R.B. performed research; J.H.A., R.D.G., N.R.H., D.Y.B., and C.T.B. contributed new reagents/analytic tools; J.W.S., and P.A.V. analyzed data; and J.W.S., and E.M. Furst wrote the paper.

The authors declare no conflict of interest.

This article is a PNAS Direct Submission.

Freely available online through the PNAS open access option.

[1]To whom correspondence should be addressed. E-mail: furst@udel.edu.

This article contains supporting information online at www.pnas.org/lookup/suppl/doi:10.1073/pnas.1206915109/-/DCSupplemental.

ary repulsion/attraction) change both the kinetics of structure growth and the eventual arrested structure, respectively. Chiefly, the sedimentation rate of micron-sized structures in water scales as r^{d_f-1} where r is the characteristic size of the aggregate and d_f is its fractal dimension (21). Therefore, aggregation processes, in which r grows with time and coarsening processes, in which d_f does the same, naturally enhance sedimentation on Earth. In the microgravity environment, the characteristic sedimentation rate for colloids is one million times smaller than the terrestrial rate. Therefore, no such boundary mediated kinetic or structural changes occur.

The present study follows a protocol similar to that of Promislow and Gast (14, 15) for which a dilute suspension of polystyrene particles seeded with magnetic nanodomains is subjected to a spatially uniform magnetic field pulsed off and on at a fixed frequency. The formation of columnar and ellipsoidal structures are observed and their widths measured through the analysis of video micrographs. The suspension may experience two distinct modes of growth: a thermal regime in which the width of aggregates increases with a subunity exponent of time (*approximately* 0.3) and a ballistic regime in which the width of aggregates increases with a superunity exponent of time (*approximately* 1.5). In the former, the suspension forms a sample-spanning network (percolates) which ripens through aggregation in the direction normal to the applied field. In the latter, compact domains of particles advect through sample meeting tip-to-tip and condensing. The sample-spanning state always precedes condensation, which only occurs under particular experimental conditions. Next, we present an analysis of these results and show that a clear demarcation between the kinetic regimes of phase separation is given by a relationship between the imposed field strength, H and the pulse frequency, ν. In particular, the quantity $\nu H^{4/3}$ must not exceed a critical value to observe ballistic condensation. Lastly, we discuss the conclusions of this work, including potential applications for the field-directed assembly of colloids and nanoparticles.

Results and Discussion

Dilute suspensions (<1% particles by volume) of superparamagnetic polystyrene spheres (radius 525 nm) in microgravity are subjected to magnetic fields pulsed with varied frequencies and field strengths. Fig. 1*A* depicts micrographs of four characteristic suspension structures observed in these experiments. These images are captured under bright field illumination so that dark regions are particle rich and light regions are particle poor. When the magnetic field is off, the particles assume an isotropic structure in which any isolated region of the suspension is indistinguishable from another (top-left). Within the first seconds after the field is applied, the particles experience attractive, interparticle forces oriented parallel to the magnetic field and form chains that aggregate laterally, forming a percolated, gel-like structure (top-right) (18). Given longer duration under the pulsating field (*approximately* 10 min) all suspensions undergo a coarsening transition as fluctuations in the orientations of nearby chains produce an attractive, chain-chain interaction force (bottom-left) (3). In some cases in which the magnetic field strength and pulse frequency are compatible, the coarsening transition changes. The suspension condenses, and elongated droplets of magnetic particles result. This process is apparent after approximately an hour in the pulsed field and accelerates as time proceeds. Pulsing of the field leads to formation of large columnar droplets with particles likely ordered on a body-centered-tetragonal lattice (bottom-right) (6, 7).

Fig. 1*B* compares the structures that emerge in two experiments with identical suspension volume fraction (6.5×10^{-3}) and field strength (1,500 A/m) but different pulse frequencies (0.66 Hz and 20 Hz). One column of pixels from the center of the recorded microscopy images is extracted and traced through time in order to gain a sense of the rate of coarsening in the suspension. In each case we observe a long period over which a fibrous, but system-spanning structure evolves. However, in the top half of the figure (0.66 Hz oscillation) after roughly 60 min, the suspension collapses, contracts from the sample walls in the field direction, and forms large dense domains of particles that interact and coalesce. In the bottom half of the figure (20 Hz oscillation), it appears that coarsening also slows, but the system spanning network remains stable and does not collapse into a condensed phase.

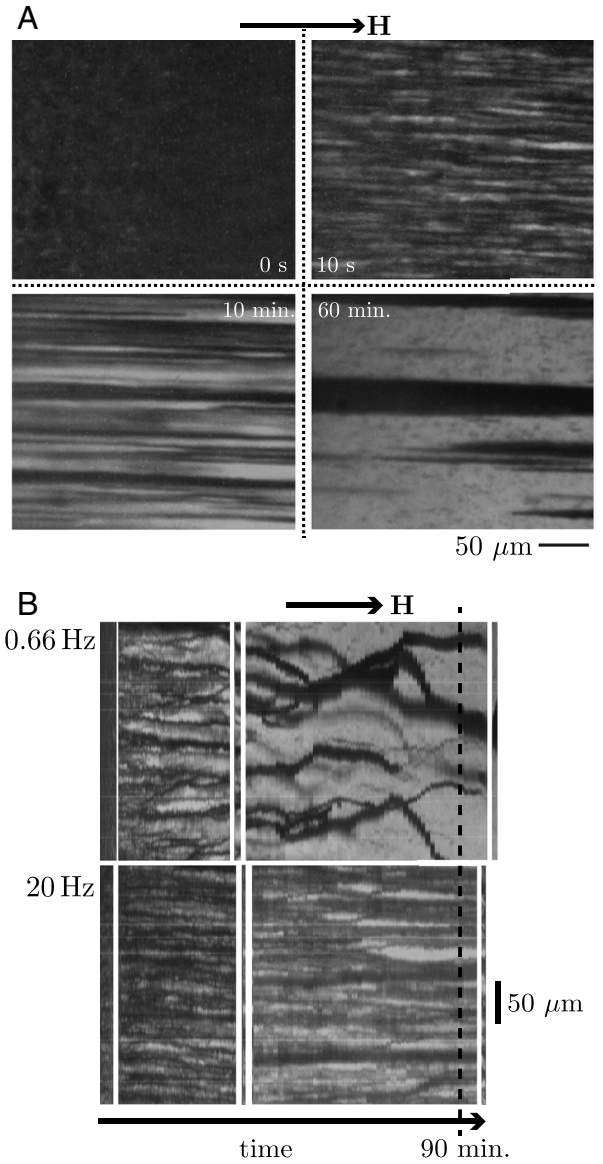

Fig. 1. (*A*) A suspension of 0.65% particles by volume is subject to a 1,500 A/m field oscillated at 0.66 Hz. Depicted are microscopy images of the suspension before the field is applied (top-left), after 10 s in the field during which particles begin to chain (top-left), after 10 min in the the field when chains aggregate laterally to form a percolated network (bottom-left) and after 1 h in the field when coalesced elongated domains interact and aggregate (bottom-right). (*B*) Here we compare structures emerging in time (spatio-temporal) as the suspension microstructure develops by choosing a vertical slice through the video micrograph a single pixel wide and plotting consecutive slices in time adjacent to one another. Each slice is separated by approximately 200 s in time. The white spaces in between segments correspond to periodic refocusing of the optics. Above: a suspension of 0.65% particles by volume, subject to a 1,500 A/m field oscillated with a frequency of 0.66 Hz condenses into columnar phases in the pulsed magnetic field. Below: a suspension 0.65% particles by volume, subject to a 1,500 A/m field oscillated with a frequency of 20 Hz fails to condense in the pulsed magnetic field.

When the suspension condenses, rapid and directed motion of the particle droplets (i.e., ballistic motion) occurs. We hypothesize that the droplets are reorganizing to minimize the magnetic interaction energy much the way bar magnets thrown at random onto a flat surface will rapidly reorient and translate to find a stable mechanical equilibrium. The pulsating field gives the droplets fluidity which prevents the system from arresting in a metastable state. The driving force may be inferred from observation of pairs of condensed ellipsoids meeting tip-to-tip, a magnetically favorable configuration, and merging (see Fig. 2). A rapid rearrangement of the merged condensate is seen during which mass transfer via surface motion of particles acts to form a new, wider droplet that is shorter than the sum of the lengths of the two premerged domains. Presumably, the surface energy and magnetic volume polarization are locally minimized by this swelling and shrinking of the material. Furthermore, smaller structures (individual particles, chains, and remnants of the percolated network) are absorbed on collision with the condensed ellipsoids increasing the ellipsoid size and magnetic moment. Ballistic coalescence favors the growth of large aggregates while depleting free particles in suspension.

The dipole–dipole interaction potential between a pair of paramagnetic colloidal particles labeled α and β and treated as point dipoles is

$$U_{\alpha\beta} = \frac{1}{4\pi\mu_0 r_{\alpha\beta}^3}(\mathbf{I} - 3\hat{\mathbf{r}}_{\alpha\beta}\hat{\mathbf{r}}_{\alpha\beta}) : \mathbf{m}_\alpha\mathbf{m}_\beta,$$

where μ_0 is the vacuum permeability, $r_{\alpha\beta}$ is the distance between the particles and $\hat{\mathbf{r}}_{\alpha\beta}$ is the unit vector connecting the centers of the particles and colon signifies the double-dot-product (22). In the presence of a magnetic field, $\mathbf{H}$, a particle, denoted α, polarizes to acquire the magnetic moment $\mathbf{m}_\alpha = \frac{4}{3}\pi a^3\mu_o\chi\mathbf{H}$, where χ is the particle magnetic susceptibility and a is the particle radius.

Newton's second law (the Langevin equation) written for particle α in a monodisperse MR fluid is

$$\frac{4}{3}\pi\rho a^3\ddot{\mathbf{x}}_\alpha = -6\pi\eta a\dot{\mathbf{x}}_\alpha - \left(\frac{4\pi a^6\mu_0\chi^2H^2}{9}\right)\nabla_\alpha\left(\sum_{\beta\neq\alpha}\frac{u_{\alpha\beta}}{r_{\alpha\beta}^3}\right) + \mathbf{F}_\alpha^B,$$

where $\mathbf{x}_\alpha$ is the position of the center of particle α, ρ is the particle density, $u_{\alpha\beta} = (\mathbf{I} - 3\hat{\mathbf{r}}_{\alpha\beta}\hat{\mathbf{r}}_{\alpha\beta}) : \mathbf{HH}/H^2$, and $\mathbf{F}_\alpha^B$ is the stochastic Brownian force on the particle (21). Here we assume the hydrodynamic forces on the particle are due solely to the Stokes drag (i.e., there are no hydrodynamic interactions).

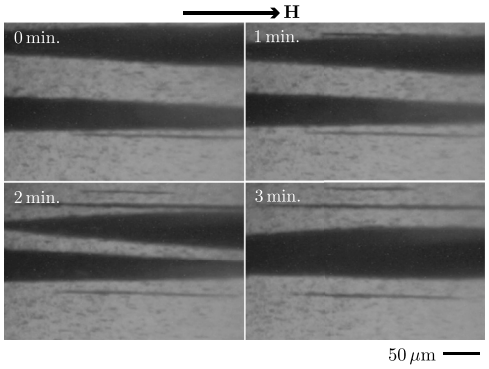

Fig. 2. Two columnar domains meet tip-to-tip and merge forming a condensed droplet. The elapsed time is approximately 3 min so that the aggregates are moving with a relative velocity of more than 0.3 μm/s. As they are at least 50 μm wide, the rms speed such aggregates might acquire from thermal motion is orders of magnitude smaller. The condensation is likely an athermal process. The concentration of particles is 0.56% by volume. The field strength is 1,500 A/m and the frequency is 0.66 Hz. Movie S1 depicts the collapse of this suspension.

The Langevin equation prefigures several characteristic time scales:

$$\tau_P = \frac{2\rho a^2}{9\eta} = 1.4\times10^{-8}\ \text{s},$$

for viscosity to slow an unforced particle,

$$\tau_D = \frac{6\pi\eta a^3}{kT} = 0.54\ \text{s},$$

for a particle to diffuse a distance equivalent to its radius and

$$\tau_B = \frac{72\eta}{\mu_0\chi^2H^2} \approx 5.9\times10^{-3}\ \text{s} - 2.4\times10^{-2}\ \text{s},$$

for two particles aligned normal to the field and at contact to be driven one radius apart by the magnetic field. Central to these scales is the dependence on the particle size, a. Notably, the time scale for dipole–dipole interactions, τ_B, is independent of the particle size. For the *approximately* 0.5 μm radius particles employed in these experiments, inertial relaxation (τ_P) is immediate while Brownian motion and field induced motion occur over comparable time scales. The dimensionless group

$$\lambda = \frac{\tau_D}{\tau_B} = \frac{\pi\mu_0 a^3\chi^2H^2}{12kT} \approx 20\text{–}110 \qquad \textbf{[1]}$$

characterizes the strength ratio of dipole–dipole forces driving particle coalescence to entropic, restoring forces which actively resist fractionation. Strong magnetic interactions are indicated by $\lambda \gg 1$ while Brownian motion dominates when $\lambda \ll 1$. Here we provide representative values spanning the range of parameters examined on the International Space Station (ISS).

It has been observed for dilute ER fluids in a *steady* field that $\lambda \geq 10$ leads to a rigid, percolated network possessing a sizable yield stress and a typical shear viscosity orders of magnitude larger than that of the solvent (1). Although the predicted equilibrium state of such materials is a condensed phase with body-centered-tetragonal order in coexistence with a dilute fluid phase, the structural transitions accompanying phase separation appear to arrest long before equilibrium is reached (3, 6, 7). The reason for this arrest can be understood by renormalizing the diffusive and magnetic time scales. The characteristic time scale for thermal rearrangement grows with the aggregate size as this requires collective motion particles in the aggregate. The time scale for the magnetic interactions may decrease as the magnetic interaction arises from volume polarizability. Consequently, there comes a point where thermal restructuring of the suspension is no longer feasible and the particles become frozen in an athermal state far from equilibrium (i.e., increasing the size of aggregates is functionally equivalent to decreasing the temperature).

In the presence of the pulsed field, however, there is an additional time scale

$$\tau_O = \frac{2}{\nu} \approx 0.1\ \text{s}\text{–}3\ \text{s}$$

reflecting the period over which the field is off and free Brownian motion relaxes the suspension structure. Comparing this to the time required for a particle to diffuse a single particle radius, we find that $\tau_D/\tau_O \approx 0.2\text{–}5$ so that our experiments encompass two different dynamical regimes: one in which this ratio is small and particles have considerable time to rearrange diffusively in the field off state, and another in which it is large and particle rearrangement is inhibited. More precisely, we may define a capture radius, denoted r_c, reflecting the distance at which the

dipole–dipole interaction forces between a pair of particles $[(4\pi/3)\mu_0\chi^2H^2/r_c^4]$ are comparable to the root mean squared (rms) Brownian force accumulated over the time it takes to diffuse the capture radius $(\sqrt{2}kT/r_c)$, *viz*

$$\frac{r_c}{a} = 2^{7/6}\lambda^{1/3} \approx 6\text{–}11.$$

This quantity describes the distance a particle contacting another must move to escape the attractive magnetic potential. The time required for a particle to diffuse the capture radius scales as $6\pi\eta a r_c^2/kT$. Therefore, the importance of the pulsed field frequency is more properly evaluated by comparing this time to τ_O so that

$$\xi = \left(\frac{\tau_D}{\tau_O}\right)\left(\frac{r_c}{a}\right)^2 \approx 6\text{–}620. \qquad [2]$$

It is apparent that ξ is the key parameter in determining whether a suspension relaxes to its equilibrium state in the pulsed field or arrests as a heavily cross-linked network. In Fig. 3*A* we plot a phase diagram of observed final states (collapsed vs system-spanning) as a function of λ and ξ and observe that there is a sharp transition from collapsed to system-spanning structures.

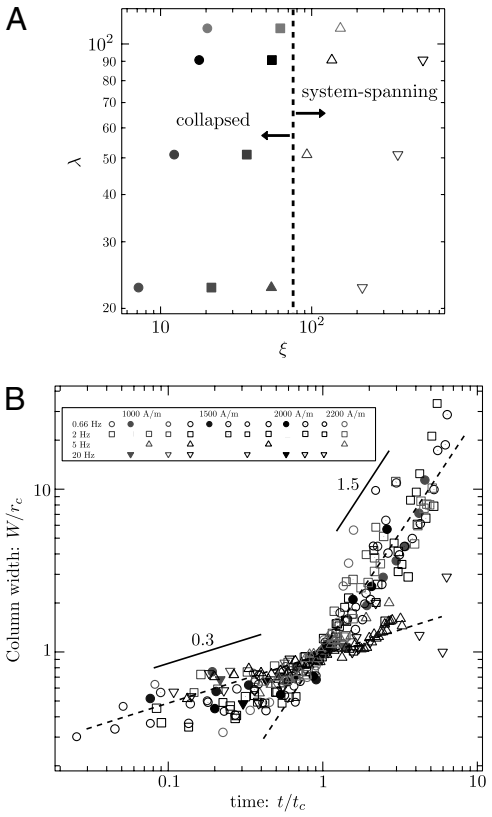

Fig. 3. Depicted in (*A*) is a phase diagram of observed final suspension state as a function of λ: the magnetic potential made dimensionless on the thermal energy and ξ: the product of the time required to diffuse the magnetic capture radius and the field oscillation frequency. Solid symbols correspond to the observation of condensed elongated droplets at experiments end while open symbols correspond to the persistence of a dense, sample-spanning network. Plotted in (*B*) is the width of aggregates as a function of time rescaled to collapse the results onto one of two master curves for sample spanning and condensation. The scheme of symbol color and shape is such that (red, blue, black, green) represent field strengths of (1,000; 1,500; 2,000; 2,200 A/m), (circle, square, up triangle, down triangle) represent frequencies of (0.66, 2, 5, 20 Hz) and (thin, filled, dot, thick) symbols represent volume fractions of (4.0×10^{-3}, 4.8×10^{-3}, 5.6×10^{-3}, 6.5×10^{-3}).

Over a period of at least an hour and up to six hours in the magnetic field only suspensions with $\xi < 70$ condense into columnar structures. This observation is robust with respect to variation in field strength (λ) and concentration (ϕ). However, there are four contradictory experiments with $\xi < 70$ but no apparent condensation—at 0.66 Hz with volume fractions of 0.40×10^{-3} and 0.65×10^{-3} with $H = 1{,}000$ A/m and at 0.66 Hz with volume fractions of 0.48×10^{-3} and 0.65×10^{-3} and $H = 1{,}500$ A/m. The observation times for these particular experiments were limited by the ISS crew schedule and were at least 10 min (*approximately* 15%) and up to 120 min (*approximately* 60%) shorter than others at similar field strengths and frequencies. In these exceptional cases, although condensation was not directly observed, the suspension structure coarsened significantly. Presumably, given more time condensation would occur in these cases too.

As a means of directly comparing experiments, we define t_c as the time at which the average measured column width exceeds the magnetic capture radius. In Fig. 3*B*, the column width normalized by r_c and plotted as a function of time rescaled by t_c demonstrates universal growth kinetics over all the experiments resulting in condensation. Chiefly, in the sample-spanning regime, $t < t_c$, we find that the aggregate width grows as a power law in time with a subunity exponent (*approximately* 0.3) which is indicative of a diffusion limited process (23). The characteristic structural wavelength during diffusive coarsening is known to grow with power laws that vary depending on the mode of diffusion: bulk diffusion $t^{1/3}$ and surface diffusion $t^{1/4}$ (24). While physically, we suspect that surface diffusion dominates the coarsening of the sample-spanning network as surface particles are the most mobile, a power law fit to the data for $t < t_c$ cannot distinguish between the two modes. In the athermal regime, $t > t_c$ and $\xi < 70$, another power law is apparent with a super-unity exponent (*approximately* 1.5) when we observe ballistic coalescence (i.e., coalescence driven by the magnetic interactions among droplet aggregates). What determines this power law and why the transition occurs when the columns grow larger than the magnetic capture radius remain open questions. However, work on the late stages of spinodal decomposition suggest that the transition from diffusive ($t^{1/3}$) to ballistic (t) coarsening may be anticipated during a fluid-fluid phase transition (25). For experiments in which the dimensionless parameter ξ was too large (>70) we see that slower growth rate persists well beyond t_c. The structure is kinetically arrested and can grow only through further chain-chain fluctuation interactions.

A long pursued goal of colloid science is the directed self-assembly of novel structured materials (26, 27). The rational design of exotic material properties calls on a detailed understanding of thermodynamics and mechanics as well as other disciplines (among them hydrodynamics and electrodynamics). Ultimately, when the desired and thermodynamically stable structure can be identified, a direct route to phase separation may be hampered by various kinetic limitations—as with electrorheological and magnetorheological suspensions. In a steady external field, symmetry of the dispersion is broken giving it tremendous rigidity that localizes particle motion (28). The kinetic barrier might be subverted by giving the suspension a unique microstructure before turning the field on, though what this structure would be or how it could be achieved is presently unpredictable. Instead, we eliminate the barrier by turning the field off and remobilizing the particles. In the field off state, symmetry of the dispersion is partially restored, the gel loses rigidity and relative diffusion of the colloids is enhanced. Repetition of this process drives the suspension into its desired equilibrium state.

We summarize this general process by depicting the phase diagrams for nonequilibrium and equilibrium states in dipolar hard-spheres in Fig. 4. The two regimes are connected by a path representing the nonequilibrium process of pulsing the field.

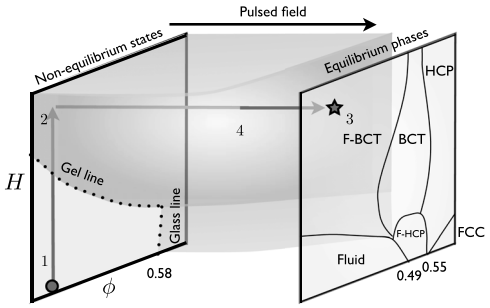

Fig. 4. Depicted are the kinetically arrested regions of the dipolar hard-sphere phase diagram and the equilibrium phases for dipolar hard-spheres. The InSPACE experiments enter the kinetically arrested region when the field is first applied—progressing from (1) to (2). The nonequilibrium process of pulsing the field, however, allows the suspension to relax and proceed to form the desired equilibrium structure—progressing from (2) to (3). The surfaces in blue represent the resection of the barriers driving kinetic arrest as the annealing process proceeds. The transition from thermal to athermal phase separation kinetics corresponds to the point labeled (4).

Given a steadily applied magnetic field, a dilute paramagnetic dispersion gels spontaneously. However, pulsing the field at the proper rate allows the dispersion to traverse a "reaction coordinate." The amorphous solid relaxes to equilibrium—columns of body-centered-tetragonal crystals. In other colloidal materials, traversals through the phase diagram and across the glass and gel lines reflecting kinetic hindrance to directed assembly may also be achieved through measured, periodic variation of driving forces. We have demonstrated that nonequilibrium processes may be engineered to drive escape from kinetically arrested (nonequilibrium) states. How to rationally and generically design such processes remains a fruitful area of inquiry.

During the directed assembly of paramagnetic colloidal particles by pulsed magnetic fields, we observe the transition from a sample-spanning network to condensed droplets on varying the pulse frequency and magnetic field strength. The characteristic percolated structure formed by the entanglement of chains of paramagnetic colloids drawn together by dipolar interactions is broken through annealing. Allowing the suspension microstructure to relax with the field off long enough for the percolated structure to dissolve, leads to a more condensed microstructure when the field is turned on again. Repetition of this pulse results in a condensed microstructure similar to the equilibrium thermodynamic state for a hard-sphere dipolar fluid: a condensed phase of body-centered-tetragonal crystals in coexistence with a dilute fluid phase. The maximum pulse frequency at which this transition occurs scales inversely with a fractional power of the field strength $\xi \sim \nu_{\max} H^{4/3} = \text{constant}$. A dependence of this transition on particle size was untested but may be inferred from analysis of the same relaxation time scales so that $\nu_{\max} \sim a^{-5}$ as well. While past studies have observed large, condensed aggregates in suspensions driven by dipolar interactions (14, 15), a combination of gravitational stresses and boundary effects lead to arrest of such structures. The microgravity environment reveals the dynamics of growth within the condensation regime—a temporal transition from slow, thermal growth to rapid, athermal growth is observed.

Although the InSPACE-2 apparatus is incapable of characterizing the detailed structure of the condensed columnar phase, the relaxation of columns on cessation of magnetic field displays buckling indicative of an anisotropic compressibility and consistent with body-centered-tetragonal crystals. As with other experimental studies of colloids in micro-gravity (29, 30), the results of the InSPACE-2 experiments show that in kinetically arrested systems, the role of gravitational compression is profound. However, through better understanding of the equilibrium and out-of-equilibrium phase behavior in the absence of gravitational stresses, dipolar fluids may be harnessed in the creation of unique materials and electro-mechanical devices.

Materials and Methods

The MR fluid samples consist of colloidal particles (radius 525 nm, CV <3%; Dynabead MyOne, Invitrogen) suspended in ultra-pure water (conductivity 5.5×10^{-6} S/m) and stabilized by electro-static interactions. The particles are composed of highly cross-linked polystyrene embedded with evenly distributed iron oxide nanoparticles. The magnetic moments of the monodomain nanoparticles are randomly aligned in the polymer matrix, giving the latex particles zero remnant magnetization. The particle susceptibility characterized by a vibrating sample magnetometer is $\chi = 1.4$.

Glass vials (dimensions: 2 mm wide, parallel to magnetic field; 0.2 mm deep; *approximately* 50 mm long, Wale Apparatus) of the MR fluid with particle volume fractions $\phi = 4.0$, 4.8, 5.6 and 6.5×10^{-3} were flown on Space Transportation System-120 to the ISS. The glass vials were held rigid in custom fabricated aluminum sample holders. Samples were prepared and stowed relatively soon before the shuttle launch in order to ensure that compaction of the particles under gravity did not lead to an irreversibly aggregated sediment. Additionally, evaporation of solvent was observed in the form of a bubble in the some sample vials. The rate of evaporation was less than 200 nL/month; change in particle concentration due to evaporation and irreversible, terrestrial aggregation was estimated to be no more than 10% by examining the saturation of micrographs of the sample vials taken before the magnetic field was applied.

Experiments were performed onboard the ISS in the Microgravity Science Glovebox as part of the project InSPACE-2 (Investigating the Structure of Paramagnetic Aggregates from Colloidal Emulsions 2). The MSG experimental setup, depicted in Fig. 5, included a Helmholtz coil surrounding a sample vial held within a rigid sample holder, an avionic setup to control the magnitude of the magnetic field, H, and pulse frequency, ν, and an optical assembly consisting of two digital video (DV) cameras (Hitachi HV-C20, 768×494 pixels, 30 fps) and a fiber optic light source. The two cameras were positioned perpendicular and parallel to the direction of the magnetic field. This configuration enabled observation of a suspension in two different orientations: a lateral view (denoted RT) in which the magnetic field lines and extended aggregates are collateral with the horizontal field of view (0.361 mm × 0.259 mm); and a straight view (denoted ST) in which the magnetic field lines and and aggregates extend normal to the field of view (0.347 mm × 0.256 mm). The data presented in this paper were taken using the lateral (RT) view.

The initially quiescent and dispersed suspensions were subjected to a pulsed magnetic field (strength $H = 1{,}000$; 1,500; 2,000; 2,200 A/m) with symmetric duty cycle (frequency $\nu = 0.66$, 2, 5, 20 Hz) using a pair of Helmholtz coils. Astronauts aboard the ISS focused the DV cameras (either the ST or RT view) on the sample vial. Throughout the experiment, the camera was refocused periodically to provide the clearest possible view of developing structures. The duration of experiments ranged from one hour to as long as six hours depending in part on the availability of the MSG facility and

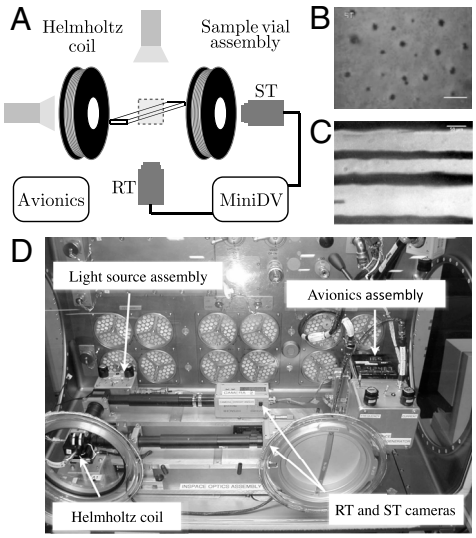

Fig. 5. (*A*) Schematic of the flight experiment. Sample images are shown taken from the (*B*) ST camera view, which is parallel to the external field, and the (*C*) RT camera, which is perpendicular to the field. (*D*) The experiment in the ISS Microgravity Sciences Glovebox.

the ISS scientific crew. The typical experimental run lasted ninety minutes. The video micrographs were subsequently analyzed frame-by-frame using MATLAB software for image analysis. The characteristic feature size of colloidal aggregates was measured in the direction normal to the field by counting the pixels of video darkened by the aggregate. Employing this method with the Hitachi HV-C20 camera gives a minimum resolution to the measurements of 0.5 μm.

ACKNOWLEDGMENTS. Support from NASA (grant nos. NAG3-1887, NAG3-2398, NAG3-2832 and NNX07AD02G) is gratefully acknowledged.

1. Halsey TC (1992) Electrorheological fluids. *Science* 258:761–766.
2. Klingenberg D (2001) Magnetorheology: Applications and challenges. *AIChE J* 47:246–249.
3. Halsey TC, Toor W (1990) Fluctuation-induced couplings between defect lines or particle chains. *J Stat Phys* 61:1257–1281.
4. Hagenbüchle M, Liu J (1997) Chain formation and chain dynamics in a dilute magnetorheological fluid. *Appl Opt* 36:7664–7671.
5. Furst EM, Gast AP (1998) Particle dynamics in magnetorheological suspensions using diffusing-wave spectroscopy. *Phys Rev E* 58:3372–3376.
6. Dassanayake U, Fraden S, van Blaaderen A (2000) Structure of electrorheological fluids. *J Chem Phys* 112:3851–3859.
7. Hynninen A-P, Dijkstra M (2005) Phase diagram of dipolar hard and soft spheres: Manipulation of colloidal crystal structures by an external field. *Phys Rev Lett* 94:138303.
8. Grant MC, Russel WB (1993) Volume-fraction dependence of elastic moduli and transition temperatures for colloidal silica gels. *Phys Rev E* 47:2606–2614.
9. Verduin H, Dhont JKG (1995) Phase diagram of a model adhesive hard-sphere dispersion. *J Colloid Interface Sci* 172:425–437.
10. Segré PN, Prasad V, Schofield AB, Weitz DA (2001) Glasslike kinetic arrest at the colloidal-gelation transition. *Phys Rev Lett* 86:6042–6045.
11. Bailey AE, et al. (2008) Spinodal decomposition in a model colloid-polymer mixture in microgravity. *Phys Rev Lett* 99:205701.
12. Lu PJ, et al. (2008) Gelation of particles with short-range attraction. *Nature* 453:499–503.
13. Eberle APR, Wagner NJ, Castaneda-Priego R (2011) Dynamical arrest transition in nanoparticle dispersions with short-range interactions. *Phys Rev Lett* 106:105704.
14. Promislow JHE, Gast AP (1996) Magnetorheological fluid structure in a pulsed magnetic field. *Langmuir* 12:4095–4102.
15. Promislow JHE, Gast AP (1997) Low-energy suspension structure of a magnetorheological fluid. *Phys Rev E* 56:642–651.
16. Cutillas S, Bossis G, Cebers A (1998) Flow-induced transition from cylindrical to layered patterns in magnetorheological suspensions. *Phys Rev E* 57:804–811.
17. Halsey TC, Toor W (1992) Structure of electrorheological fluids. *Phys Rev Lett* 65:2820–2823.
18. Fermigier M, Gast AP (1992) Structure evolution in a paramagnetic latex suspension. *J Colloid Interface Sci* 154:522–539.
19. Lemaire E, Grasselli Y, Bossis G (1992) Field induced structure in magneto- and electrorheological fluids. *J Phys II France* 2:359–369.
20. Grasselli Y, Bossis G, Lemaire E (1994) Structure induced in suspensions by a magnetic field. *J Phys II France* 4:253–263.
21. Russel WB, Saville DA, Schowalter WR (1989) *Colloidal Dispersions* (Cambridge University Press, Cambridge).
22. Landau LD, Lifshitz EM, Pitaevskii LP (1984) *Electrodynamics of Continuous Media* (Elsevier Butterworth-Heinemann, Oxford), 2nd edition.
23. Witten TA, Sander LM (1981) Diffusion-limited aggregation, a kinetic critical phenomenon. *Phys Rev Lett* 47:1400–1403.
24. Sethna JP (2006) *Statistical Mechanics: Entropy, Order Parameters and Complexity* (Oxford University Press, Oxford).
25. Siggia E (1979) Late stages of spinodal decomposition in binary-mixtures. *Phys Rev A* 20:595–605.
26. Dinsmore AD, Crocker JC, Yodh AG (1998) Self-assembly of colloidal crystals. *Curr Opin Colloid Interface Sci* 3:5–11.
27. Grzelczak M, Vermant J, Furst EM, Liz-Marzán LM (2010) Directed self-assembly of nanoparticles. *ACS Nano* 4:3591–3605.
28. Chaikin PM, Lubensky TC (2000) *Principles of Condensed Matter Physics* (Cambridge University Press, Cambridge).
29. Zhu J, et al. (1997) Crystallization of hard-sphere colloids in microgravity. *Nature* 387:883–885.
30. Cheng Z, Chaikin PM, Zhu J, Russel WB, Meyer WV (2001) Crystallization kinetics of hard spheres in microgravity in the coexistence regime: Interactions between growing crystallites. *Phys Rev Lett* 88:015501.